The Local Minima Method (LMM) of Pharmacophore Determination: A Protocol for Predicting the Bioactive Conformation of Small, Conformationally Flexible Molecules

David A. Demeter,*,‡ Herschel J. R. Weintraub,† and James J. Knittel§

The R.W. Johnson Pharmaceutical Research Institute, Route 202, P.O. Box 300, Raritan, New Jersey 08869, Helios Pharmaceuticals, Inc., 9800 Bluegrass Pkwy, Louisville, Kentucky 40299, and University of Cincinnati, Division of Pharmaceutical Sciences, College of Pharmacy, Cincinnati, Ohio 45267-0004

Received April 10, 1998

Software has been developed for potential energy surface analysis and the local minima method of pharmacophore determination.[1] LMM is rigorous and systematic and employs multiple conformations which are the local minima from the potential energy surface of each compound in the data set. It produces a series of possible pharmacophores from a postulated set of pharmacophore elements. The best pharmacophore is then determined by performing a comparative molecular field analysis (CoMFA) on each one. The pharmacophore which produces the most self-consistent model is deemed the best. Local minima on the gas-phase potential energy surface are shown to be a reasonably close approximation to protein bound conformations, and these conformations can be found through systematic conformational searches followed by minimization of the local minima. LMM was used to develop a 3D-QSAR model for dopamine β-hydroxylase (DBH) inhibitors which was highly predictive (predictive $R^2 = 0.71$ and standard error of predictions $= 0.41$). The model predicted that the phenyl and thienyl series of inhibitors were acting as bioisosteres. Examination of compounds overlayed in the model indicated a possible hydrogen bond acceptor in the DBH active site. Three tyrosine residues previously labeled by mechanism based inhibitors may be acting as the acceptor and therefore represent excellent candidates for site-directed mutagenesis studies.

INTRODUCTION

Dopamine β-hydroxylase (DBH; EC 1.14.17.1) is a tetrameric complex containing two copper atoms per catalytic subunit.[2] It is found in the adrenal medulla[3] as well as the sympathetic nerve endings.[4] The oxidized form containing Cu(II) is reduced by ascorbate to give the catalytically active Cu(I) form of DBH.[5] The chemistry of the enzyme occurs via direct metal catalysis with no cofactor required,[6] and it is also not very substrate specific.[7] DBH catalyzes the conversion of dopamine to norepinephrine in the catecholamine biosynthetic pathway,[8] thus providing a way to regulate catecholamine production.[9] Studies have correlated high levels of norepinephrine with high blood pressure[10] and congestive heart failure.[11] Therefore, inhibitors of dopamine β-hydroxylase are of interest as potential therapeutic agents for the treatment of these cardiovascular diseases.[12] A number of approaches have been tried for creating inhibitors of DBH.[13]

One approach, by Kruse et al.,[14−16] has been the successful development of 1-(phenylalkyl)imidazole-2(3*H*)-thiones (Table 1, rows 13−56) at Smith Kline & French Laboratories (SKF). They have been shown to be competitive multisubstrate inhibitors of DBH with respect to tyramine and oxygen while being uncompetitive with ascorbic acid. The phenyl moiety was designed to bind to the substrate phenyl site, while the imidazole-2(3*H*)-thione ring was meant to act as an oxygen mimic, thus binding at the oxygen binding sight. Under the conditions of kinetic assays, the compounds were believed to exist predominantly in the neutral, un-ionized form. Data on two additional, related series of compounds have also been published. One of the sets contained six different 1-(pyridylmethyl)imidazole-2(3*H*)-thiones,[17] while the other set of benzyl-substituted compounds was synthesized where the imidazole-2(3*H*)-thione ring was varied.[18] These compounds were not considered in this study.

Bioisosteric replacement of the phenyl group with thiophene[19] by McCarthy et al.[20] at Marion Merrell Dow Inc. (MMD) resulted in a series of 11 1-(thienylalkyl)imidazole-2(3*H*)-thiones which were potent competitive inhibitors of dopamine β-hydroxylase (Table 1, rows 1−12). The structure−activity relationships of the two different series showed an interesting trend. The 4-hydroxyphenyl and thiophene derivatives were equipotent when Y was CH_2 or $(CH_2)_3$. However, the thiophene derivatives exhibited their best potency when Y was $(CH_2)_2$, while the 4-hydroxyphenyl derivatives exhibited their worst potency. It was demonstrated via an active analogue approach that the two series could adopt similar conformations, but this did not explain the differences in their activity trends.

The primary amino acid sequences for mouse,[21] rat,[22] bovine,[23] and human[24] DBH have been determined. The mouse DBH showed an amino acid identity of 87%, 80%, and 79% with the rat, bovine, and human sequences, respectively.[21] Several studies employing mechanism based inhibitors have labeled amino acid residues which are presumed to be in the substrate binding site. These include Tyr 216,[25] His 249,[28] Tyr 357,[26] His 398,[27] and Tyr 477[28] (amino acid residue from bovine sequence numbering from

* To whom correspondence should be addressed. E-mail: demeterd@prius.jnj.com.
‡ R. W. Johnson Pharmaceutical Research Institute.
† Helios Pharmaceuticals, Inc.
§ University of Cincinnati.

10.1021/ci980404z CCC: $15.00
Published on Web 10/24/1998

Table 1. Structures and Inhibitory Activity of 1-(Arylalkyl)imidazole-2(3*H*)-thione DBH Inhibitors

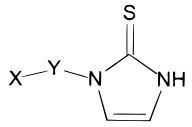

row	X	Y	IC_{50} (μM)	$-\log IC_{50}$	$-\log IC_{50}c$[a]	predictions[b]	residuals[b]
1	2-thienyl	$(CH_2)_2$	0.114	6.94	6.18	6.13	−0.05
2	3-thienyl	$(CH_2)_2$	0.130	6.89	6.13	6.04	−0.09
3	3,5-F_2-phenyl	CH_2	0.210	6.68	5.92	5.97	0.05
4	3-CH_3-2-thienyl	$(CH_2)_2$	0.491	6.31	5.55	5.56	0.01
5	3-Cl-2-thienyl	CH_2	1.000	6.00	5.24	5.02	−0.22
6	2-thienyl	$(CH_2)_3$	1.900	5.72	4.96	5.20	0.24
7	2-thienyl	$(CH_2)_4$	3.600	5.44	4.68	5.05	0.37
8	3-F-2-thienyl	CH_2	4.600	5.34	4.58	4.73	0.15
9	2-thienyl	CH_2	4.800	5.32	4.56	4.55	−0.01
10	3-thienyl	CH_2	5.300	5.28	4.52	4.34	−0.18
11	3-CH_3-2-thienyl	CH_2	6.000	5.22	4.46	5.00	0.54
12	2-furanyl	CH_2	6.300	5.20	4.44	4.87	0.43
13	4-OH-phenyl	$(CH_2)_3$	2.200	5.66	5.66	5.57	−0.09
14	4-OH-phenyl	CH_2	2.600	5.58	5.58	5.18	−0.40
15	phenyl	$(CH_2)_3$	16.000	4.79	4.79	4.91	0.12
16	4-OH-phenyl	$(CH_2)_2$	23.000	4.64	4.64	4.98	0.34
17	phenyl	CH_2	32.000	4.49	4.49	4.32	−0.17
18	4-OCH_3-phenyl	$(CH_2)_2$	68.000	4.17	4.17	4.04	−0.13
19	phenyl	$O(CH_2)_2$	87.000	4.06	4.06	4.10	0.04
20	phenyl	$S(CH_2)_2$	103.000	3.99	3.99	4.14	0.15
21	4-OCH_3-phenyl	$(CH_2)_5$	109.000	3.96	3.96	3.92	−0.04
22	phenyl		110.000	3.96	3.96	3.77	−0.19
23	4-OCH_3-phenyl	$(CH_2)_4$	152.000	3.82	3.82	3.32	−0.50
24	4-OCH_3-phenyl	$(CH_2)_3$	180.000	3.74	3.74	3.75	0.01
25	4-OCH_3-phenyl	CH_2	202.000	3.69	3.69	3.61	−0.08
26	4-OH-phenyl		370.000	3.43	3.43	3.35	−0.08
27	3,5-F_2-4-OH-phenyl	CH_2	0.074	7.13	7.13	6.59	−0.54
28	3,5-Cl_2-phenyl	$(CH_2)_3$	2.100	5.68	5.68	5.39	−0.29
29	2,3-Cl_2-phenyl	CH_2	52.000	4.28	4.28	4.37	0.09
30	4-NO_2-phenyl	CH_2	53.000	4.28	4.28	4.26	−0.02
31	4-Cl-phenyl	CH_2	96.000	4.02	4.02	4.51	0.49
32	3-CF_3-4-OH-phenyl	CH_2	121.000	3.92	3.92	3.97	0.05
33	3,5-Cl_2-4-OH-phenyl	CH_2	0.680	6.17	6.17	5.55	−0.62
34	3-F-4-OH-phenyl	CH_2	1.500	5.82	5.82	6.23	0.41
35	3-Cl-4-OH-phenyl	CH_2	2.000	5.70	5.70	5.41	−0.29
36	3,4-$(OH)_2$-phenyl	CH_2	2.200	5.66	5.66	4.99	−0.67
37	3,5-Cl_2-phenyl	CH_2	2.400	5.62	5.62	5.28	−0.34
38	3,5-F_2-phenyl	$(CH_2)_3$	4.700	5.33	5.33	5.37	0.04
39	3-F-phenyl	CH_2	5.600	5.25	5.25	5.46	0.21
40	3-Cl-phenyl	CH_2	12.000	4.92	4.92	4.82	−0.10
41	3-Br-4-OH-phenyl	CH_2	12.000	4.92	4.92	5.10	0.18
42	2,4-Cl_2-phenyl	CH_2	17.000	4.77	4.77	4.20	−0.57
43	3,4-Cl_2-phenyl	CH_2	28.000	4.55	4.55	4.86	0.31
44	3-NO_2-4-OH-phenyl	CH_2	31.000	4.51	4.51	4.65	0.14
45	3,5-F_2-4-OCH_3-phenyl	CH_2	36.000	4.44	4.44	4.78	0.34
46	3,5-Cl_2-4-OCH_3-phenyl	CH_2	47.000	4.33	4.33	4.41	0.08
47	4-F-phenyl	CH_2	47.000	4.33	4.33	4.75	0.42
48	3-CH_3-4-OH-phenyl	CH_2	49.000	4.31	4.31	4.48	0.17
49	2,3,5,6-F_4-4-OH-phenyl	CH_2	62.000	4.21	4.21	4.87	0.66
50	2,6-Cl_2-4-OH-phenyl	CH_2	75.000	4.12	4.12	4.27	0.15
51	2,5-Cl_2-phenyl	CH_2	97.000	4.01	4.01	4.27	0.26
52	2,4,6-Cl_3-phenyl	CH_2	102.000	3.99	3.99	3.80	−0.19
53	3-OH-phenyl	CH_2	148.000	3.83	3.83	4.50	0.67
54	3-OCH_3-phenyl	CH_2	157.000	3.80	3.80	4.02	0.22
55	3-NO_2-4-OCH_3-phenyl	CH_2	359.000	3.44	3.44	4.11	0.67
56	2-OH-phenyl	CH_2	580.000	3.24	3.24	3.98	0.74

[a] Corrected IC_{50} values for rows 1−12 using eq 1. [b] Values from refined model.

ref 23a). All of the labeled residues are conserved between the mouse, rat, bovine, and human sequences. The copper binding motif, HXH* (H* = His or Met),[29] is found in all of the DBH sequences. These motifs occur in three places: (248)HHM, (319)HYH, and (398)HTH. Two of these motifs contain labeled residues discussed above. Additionally, two other parts of the sequence containing closely spaced histidines have been noted.[30] They are the sequences (230)-HH and (425)HYSPH and are also conserved in the different species. The conservation of the copper binding motif in DBH from different species implies that these residues are involved in ligating the two copper atoms and is in agreement with the fact that a histidine residue has been labeled by mechanism based inhibitors in two of the motifs.

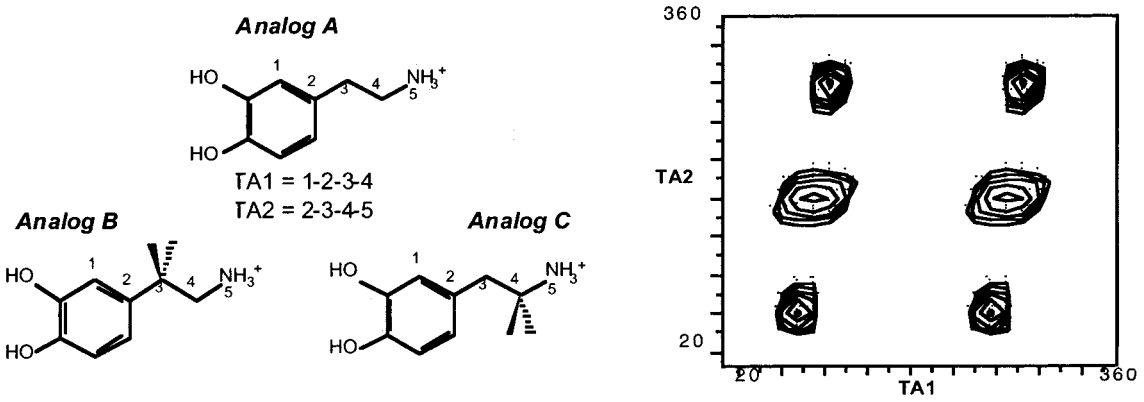

Figure 1. Potential energy surface analysis.

Spectroscopic studies of the DBH active site have been done by Pettingill et al.[31] and Blackburn et al.[32] EXAFS studies on the oxidized form of DBH led the researchers to propose a model involving two inequivalent Cu(II) sites. This result was in agreement with previous studies done by Scott et al.,[33] Blumberg et al.,[34] and McCracken et al.[35] When DBH is reduced by ascorbate the two water molecules are lost. In the model for the reduced form of DBH, one of the lost waters is replaced by an endogenous sulfur atom on a methionine residue. The other copper center now has an open coordination site which allows for the binding of the molecular oxygen substrate. Met 250 was proposed as a good candidate for providing the sulfur ligand and His 248 was proposed as one of the copper ligands. It was speculated that His 249 might also be acting as a ligand for the other copper site. Blumberg reported no change in the average copper ligand environment after reduction and no binding of any heavy atom, such as sulfur or chlorine.[34] However, the results first reported by Scott are in agreement with Blackburn's model. It was also reported by Scott, that upon the binding of 1-(3,5-difluoro-4-hydroxybenzyl)imidazole-2(3*H*)-thione, an increase in sulfur ligation was detected, thus, indicating the direct binding of the thione sulfur to at least one of the copper sites.[33]

Carbon monoxide (CO) was previously found to be a competitive inhibitor of molecular oxygen with a binding stoichiometry of one CO per two copper atoms in the reduced enzyme.[36] This demonstrated that the two Cu(I) centers in reduced DBH were inequivalent. FTIR studies with CO and tyramine showed that the binding of tyramine to DBH did not eliminate the observed CO infrared peak, while binding of the multisubstrate inhibitor 1-(4-hydroxybenzyl)imidazole-2(3*H*)-thione did eliminate the IR peak. Fluorescence studies on the CO−DBH complex showed no luminescence in the visible region. This indicated that DBH most likely possessed a mononuclear catalytic site.[37,38] Finally, the EXAFS studies produced results which were in agreement with a model indicating that CO binds to reduced DBH without displacing any of the protein-bound ligands.

Because of their inherent flexibility and small size, the 1-(arylalkyl)imidazole-2(3*H*)-thione DBH inhibitors were perfectly suited for the application of the local minima method of pharmacophore determination. The purpose of this study was to develop and test the local minima method by determining an optimal and predictive pharmacophore for DBH inhibitors of varying size. The molecules studied were picked in order to maximize the chance of finding pharmacophore models with significant statistical correlations. Therefore, only imidazole-2(3*H*)-thione oxygen mimics were considered in this study, and they were modeled in the neutral thione form.

THEORY

In the active analogue method,[39] a pharmacophore hypothesis is made based on the possible pharmacophore elements in a series of structurally diverse ligands with high activity. Following the hypothesis generation, conformations of the ligands which fit the hypothesis are determined by systematic conformational searching with distance constraints. Problems occur when no solution is found for all the molecules in the series or a large number of different conformers for each compound are found (which is the "best" conformer?). Each new hypothesis also requires repeating the conformational search process with no guarantee that a solution will be found.

In the local minima method, one postulates that the bioactive conformation of a high activity molecule is a local minimum. Thus, the number of possible conformers which must be considered is reduced to the number of minima on the potential energy surface of the molecule. The most active compound in a series is chosen as the reference compound because it contains the best pharmacophore. If the reference compound has three local minima, then there are three possible pharmacophores for a given set of hypothesized pharmacophore elements. The three minima of the reference compound are compared to the local minimum conformers of each molecule in the series, and the most similar is selected. This results in three sets of the series of ligands with the most similar shapes being aligned in three different ways. The quality of these alignments (pharmacophores) can then be evaluated using comparative molecular field analysis[40] (CoMFA) and partial least squares[41] (PLS) regression. The advantage of this method is that all of the conformational searching and minima finding are done up front only once. Multiple pharmacophore hypotheses are then made using the same data set. Also, one always gets an answer, be it a good one or a bad one. The following sections explain the LMM process in more detail.

The first step in the LMM process is to calculate the potential energy surface for every molecule in the series. The second step is to locate all the minima on each surface. A theoretical data set will be used to illustrate the basic concepts (Figure 1). Analogue A is a simple example. If

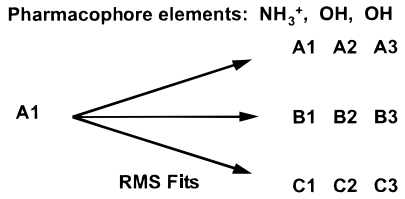

Figure 2. LMM alignment process.

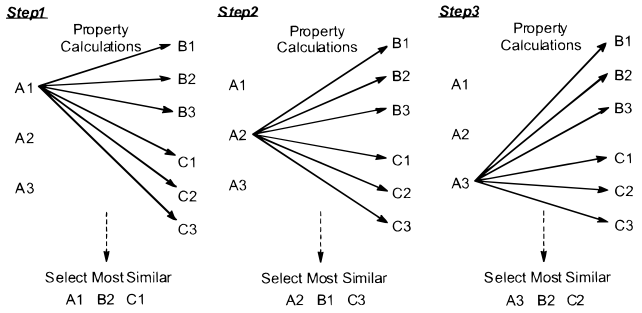

Figure 3. LMM selection process.

the two angles, TA1 and TA2, are searched at 15° increments, then each torsion angle will have 24 (360/15) possible values. All possible combinations of these sets of values give 576 (24 × 24) conformers on the energy surface. A contour plot of the two torsion angles in analogue A versus energy shows that there are only six minima on the potential energy surface. Because of symmetry, there are actually only three minima out of a total of 288 conformers. This is quite a drastic reduction in the number of conformers or important shapes of the molecule which need to be examined. The three minima represent only 1% of the possible shapes. For larger data sets, the percentage of conformers which are local minima decreases.

Let us say that analogue A is the best binding compound of a series of three compounds (analogue A, analogue B, and analogue C) and we are interested in determining the pharmacophore. All of the compounds have a protonated amine group and two hydroxyl groups on their aromatic ring system. One possible set of pharmacophore elements is simply the three distances between the heteroatoms. Each molecule in the series is found to have three local minima (A1, A2, A3; B1, B2, B3; and C1, C2, C3). Under the local minimum postulate, we now know all of the important shapes which may represent the bioactive conformations, and we are ready to proceed with the alignment process (Figure 2). In this process, all of the local minima for each compound in the series (including the reference conformers) are fit to the global minimum reference conformation using the three heteroatoms for the RMS fitting. At this point, all the conformers in the series which are local minima are aligned and ready for the selection process which produces the data sets for 3D-QSAR analyses.

The data sets are created using a property calculation and a selection rule in order to quantify the similarity between the conformers of the reference molecule and the conformers of the less active molecules (Figure 3). The property calculated is the volume of the less active conformers subtracted from the volume of the reference conformer (i.e. the difference volume, A1−B1). The selection rule for picking the most similar conformer of the less active molecule is defined as the one with the smallest difference volume which is inversely related to the amount of steric overlap.

Since analogue A is the most active compound in the series, one of its three minima must represent the best pharmacophore. Therefore, a 3D-QSAR data set must be created for each local minimum conformation of the reference molecule. The first step in the process is to perform the volume calculations using conformer A1 and the conformers of the less active molecules. The selection rule is then used to pick the most similar conformer from each of the less active molecules (B2 and C1). This creates the first data set containing A1, B2, and C1. The second and third steps involve repeating the same procedure for conformers A2 and A3, respectively. This results in three data sets which are ready for 3D-QSAR analyses using CoMFA. The data set which gives the best statistical relationship is deemed the correct pharmacophore if the correlation is strong enough. If the best correlation is only a weak one, then another pharmacophore hypothesis can be generated, and the whole process is repeated starting at the alignment phase.

It is certainly probable that the bioactive conformation of a ligand may not correspond exactly to the bottom of a gas-phase local minimum but may exist somewhere on the side of the multidimensional potential energy well. This would be caused by an induced fit due to interactions with the protein. It is not our intent to prove that all bioactive conformations are local minima. The real intent is to find a conformation which is close enough to the real answer so that the possibility of a valid pharmacophore relationship can be tested. The advantage of this method is that it reduces the number of conformations which must be considered as possible candidates. Once a valid relationship is found, the conformation of the molecule being studied can be further refined if that is deemed to be necessary to improve the 3D model.

COMPUTATIONS

The IC_{50} values for the MMD DBH inhibitors were determined using an oxygen electrode method.[20] The IC_{50}'s of the SKF inhibitors were measured by a UV absorption method[15] which produced values higher than would normally be expected based on the K_i values which were determined. While the assays were different, both used the same commercially available bovine DBH (Sigma). The same compound, 3,5-F_2-phenylmethyl (**3**), had its IC_{50} value measured in both assays. Because of the different assays plus the fact that the values were obtained from two different labs, a correction factor (eq 1) for converting MMD data values to SKF data values was determined. This was done not only so the values could be compared but also to allow the separate data sets to be combined. Calculating the correction factor and converting the data ahead of time was done instead of using an indicator variable to combine the two data sets. Some recent work indicates that the use of indicator variables in CoMFA may not be appropriate because using different values (such as 0 and 1 versus 0 and 4) can give different results.[42]

$$-\log \mathrm{IC50\ (SKF)} = -\log \mathrm{IC50\ (MMD)} - 0.76 \quad (1)$$

The first step in the LMM process was to calculate the potential energy surface for every molecule in the series (1−

26, Table 1). In this study, the structures were built in Sybyl 6.03.[43] Full geometry optimizations were done on molecules 1−26 using the Tripos force field[44] with the Powell minimizer and no electrostatics (termination_criterion = energy, min_energy_change = 0.000 01 kcal/mol, max_iterations = 1 000 000, dielectric_constant = 2.0, dielectric_function = distance, default settings were used for all other variable parameters). The rotatable bonds were then set to 180° (extended conformations). For those molecules with bad van der Waals overlaps, the appropriate torsion angle was set to a value evenly divisible by the rotatable bond angle increment. MNDO[45] atomic point charges were calculated using MOPAC 5.0[46] (TIME = 999 999, MMOK, NOINTER, default settings were used for all other variable parameters).

The energy surfaces were generated by performing systematic conformational searches using the Tripos force field with the csearch algorithm, energies, and electrostatics (reference_conformation = current, van_der_Waals_scaling_factors [general = 0.70, 1−4 = 0.70, hbond = 0.65], energy_cutoff = 9999.9 kcal/mol, dielectric_constant = 2.0, dielectric_function = distance, default settings were used for all other variable parameters). All rotatable bonds were searched from 0° to 359°. An angle increment of 15° was used for each torsion angle in molecules having 1−4 rotatable bonds. An angle increment of 30° was used for each torsion angle in molecules having five rotatable bonds. An angle increment of 60° was used for each torsion angle in molecules having six rotatable bonds.

The second step was to locate all minima on each surface. This was accomplished using the FORTRAN program, PESA 1.0 (find minima saddle path, neighbors minima saddle noprint, statistics surface saddle minima, default settings were used for all other variable parameters). It was developed as part of this study and interfaced to Sybyl using SPL (Sybyl programing language) macros. The macro interface reads the results produced by PESA for each search and creates a Sybyl database containing all the local minima from the search table. The local minima were then geometry optimized using the Tripos force field with the Powell minimizer and electrostatics. The LMM fitting and alignment procedures were then performed using maximum volume overlap as the selection rule for picking the most similar conformer. This was followed by automated CoMFA processing in order to pick the best pharmacophore. These procedures were also implemented using SPL macros. The CoMFA calculations on the steric and electrostatic fields were performed with full cross-validation, and the regions were defined automatically using the molecular volumes option (minimum_sigma = 1.0, default settings were used for all other variable parameters).

Compounds 27−56 were built in the LMM derived conformations of analogous molecules found for the best MMD pharmacophore (Model 1, Table 3) and minimized as previously described with no electrostatics. MNDO atomic point charges were calculated, and the compounds minimized again with electrostatics. The compounds were then fit to the LMM reference structure.

Potential energy surface analyses (PESA) were used to locate the minima of the compounds. The actual number of minima used in the local minima method was further reduced by filtering out those which had negative torsion angle values for the torsion angle nearest the imidazole-2(3*H*)-thione ring. This was done because the molecules possess a plane of symmetry. Filtering on this torsion angle eliminated pharmacophores which were mirror images of each other. It also sped up the calculations.

Table 2. Comparison of Small Molecule Structures Bound in Proteins to Molecular Mechanics Local Minima Determined in Vacuo

PDB code	resolution (Å)	atoms	RMS[a] (Å)	R^2_S[b]	R^2_E[c]	R^2_{avg}[d]
1MBD	1.9	70	0.999	0.85	0.70	0.77
1JET	1.2	57	0.776	0.90	0.91	0.90
1LST	1.8	25	0.290	0.96	0.98	0.97
1MMQ	1.9	69	0.530	0.95	0.77	0.86
1NSD (a)	1.8	29	0.280	0.97	0.81	0.89
1NSD (b)	1.8	39	0.272	0.97	0.91	0.94
1NSD (ref)	1.8	29	0.117	0.98	0.73	0.86
1ONE (a)	1.8	14	0.808	0.82	0.82	0.82
1ONE (b)	1.8	18	0.666	0.93	0.63	0.78
1SHA	1.5	90	0.583	0.91	0.78	0.85
2MSB	1.7	114	0.990	0.88	0.56	0.72
2RKM	1.8	47	0.697	0.91	0.93	0.92
3CLA	1.75	32	0.273	0.96	0.95	0.95
3XIS (a)	1.6	22	0.381	0.92	0.83	0.88
3XIS (b)	1.6	20	0.185	0.98	0.94	0.96
4DFR	1.7	53	1.131	0.80	0.90	0.85
4DFR (ref)	1.7	53	0.276	0.97	0.98	0.98
7ABP (a)	1.67	23	0.128	1.00	0.98	0.99
7ABP (b)	1.67	23	0.093	0.99	0.99	0.99
8TLN	1.6	41	0.829	0.90	0.93	0.91

[a] RMSD = root mean squared deviation of all C, N, O, P, and S atoms. [b] R^2_S = steric field correlation coefficient. [c] R^2_E = electrostatic field correlation coefficient. [d] $R^2_{avg} = (R^2_S + R^2_E)/2$.

A comparison for a sampling of structures from the Protein Data Bank (PDB) was performed in order to investigate our assumption that local minimum conformations are reasonably close approximations of the bioactive conformation found in ligand−protein complexes. These results are shown in Table 2. The ligands were extracted in Sybyl from each PDB structure. Some proteins had multiple ligands which were designated by the PDB entry code followed by the letter *a* or *b*. If there were identical ligands, one was denoted as *ref*. Each ligand was assigned correct atom types for the Tripos force field. Hydrogens were then added to all open valence positions, and Gasteiger−Hückel atomic point charges were calculated. A copy of the ligand was then created and minimized. Full geometry optimizations were done using the Tripos force field with the Powell minimizer and no electrostatics (termination_criterion = energy, min_energy_change = 0.00001 kcal/mol, max_iterations = 1 000 000, dielectric_constant = 2.0, dielectric_function = distance, default settings were used for all other variable parameters). The Sybyl MATCH command was used to fit all C, N, O, S, and P atoms in the minimized structure to the corresponding atoms in the X-ray structure. Steric and electrostatic COMFA fields were calculated for all the molecules using the default settings. The QSAR COMFA FIELD COMPARE command was used to calculate the steric and electrostatic field correlation coefficients of the minimized structure versus the X-ray structure. The average of the two field correlation coefficients was then determined.

Our ability to find a local minimum which is close to the protein bound structure was validated by a complete systematic search performed on two of the small molecule

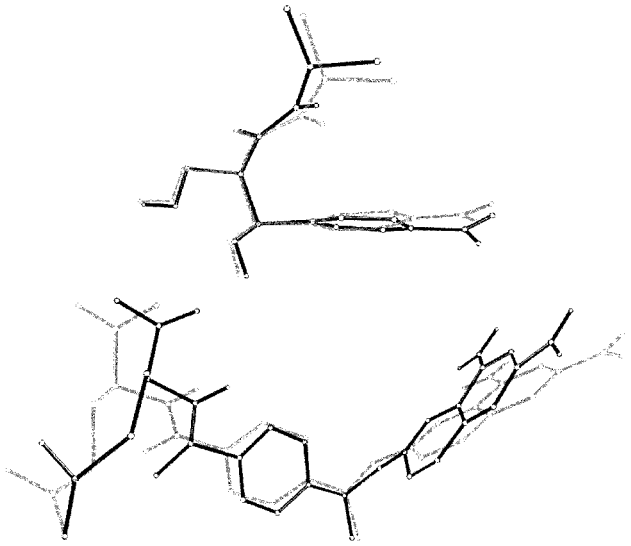

Figure 4. Overlays of local minima for chloramphenicol (above) and methotrexate (below) found via systematic conformational searching (grey) on protein bound ligand structures (black).

ligands, methotrexate from 4DFR and chloramphenicol from 3CLA (Tripos force field with the csearch algorithm, energies, electrostatics, reference_conformation = zeroed, van_der_Waals_scaling_factors [general = 0.90, 1−4 = 0.82, hbond = 0.65], energy_cutoff = 9999.9 kcal/mol, dielectric_constant = 2.0, dielectric_function = distance, default settings were used for all other variable parameters). All rotatable bonds were searched from 0° to 359°. An angle increment of 60° was used for the seven torsion angles in chloramphenicol. An angle increment of 60° was used for five of the eight torsion angles in methotrexate. The remaining three torsion angles defined by the bonds to the aniline nitrogen were sampled at an angle increment of 30°. The two carboxylic acid groups were not rotated, but their torsion angles were set to 0°. PESA was then used to locate all of the local minima on the potential energy surface (as described above). Full geometry optimizations were done on the local minima using the Tripos force field with the Powell minimizer and electrostatics (termination_criterion = energy, min_energy_change = 0.00001 kcal/mol, max_iterations = 1 000 000, dielectric_constant = 2.0, dielectric_function = distance, default settings were used for all other variable parameters). An all atom fit of each local minimum conformer to the protein bound X-ray structure was performed, and the conformer with the lowest RMS value was selected as the most similar. These overlays are shown in Figure 4.

DISCUSSION OF RESULTS

The identification and validation of useful pharmacophores is of great interest in the pharmaceutical industry. To address these needs other commercial software packages such as GASP,[47] DISCO,[48] Apex-3D,[49] and Catalyst[50] have been developed. All of these programs allow for the identification of possible pharmacophores. Pharmacophore elements are automatically identified, and then genetic algorithms and/or clique detection methods are used on multiple conformers to locate common distances between the pharmacophore elements. Multiple pharmacophore hypotheses can be derived this way. LMM is different in that it produces multiple overlays in a rigorous and systematic manner based on a given pharmacophore hypothesis rather than producing many different pharmacophores. Additional pharmacophores are produced by repeatedly applying the method starting from the alignment phase, and the pharmacophore hypothesis must be generated by the user. From this point of view, the programs mentioned above can be used as a starting point for hypothesis generation followed by a more detailed analysis using LMM. A second difference is that the LMM software streamlines the use of CoMFA as implemented in Sybyl, thus allowing for the automated generation of tens to hundreds of 3D-QSAR equations which are field based. Also, as with other pharmacophore recognition software, LMM allows the use of both ligand based and receptor based pharmacophore site points (although the examples shown here use only ligand based site points).

As part of the local minima method, the PESA software was developed in order to find minima on a molecules' potential energy surface. As implemented in the LMM software, a rigid rotor potential energy surface is generated using the CSEARCH algorithm in Sybyl. A table containing the torsion angle values and the conformer energy is used as input into PESA. The torsion angle increments need to be evenly divisible by 360, but each increment can be a different value. The adjacent points j_n to each individual point i on this N-dimensional energy surface are then systematically checked to see if any are lower in energy than the point i in question. If one point j_n is found which is lower in energy, then the point i is not a minimum. If they are all higher in energy, then the point i is a minimum. This method is very fast because only a very small percentage of points on the total energy surface are actually minima.

PESA has a limit of 10 rotatable bonds which is hard coded. It also has a limit of 3 000 000 conformers on the energy surface which can be modified. These are practical limits because the number of adjacent points on a potential energy surface increases as 3^n where n is the number of torsions. Ten rotatable bonds give 59 059 adjacent points while 11 torsions give 177 147. The theoretical maximum number of conformations from the systematic search also increases exponentially. Because of this, our definition of small conformationally flexible molecules applies to those molecules which have 10 or less rotatable bonds. Therefore, this type of analysis is not for all compounds. However, there are many types of small biologically active compounds which fall into this category. The current intent of this software is to be able to identify valid pharmacophores of small molecules in a rigorous and complete fashion. Extending the method to larger molecules will be investigated in the future. With the processing power available on todays computers and the ability to spread the computationally intensive steps over multiple processors or multiple workstations, having the ability to analyze compounds with hundreds of local minima is possible. The real difficulty will be in maintaining a rigorous and systematic search of conformational space rather than a random sampling via random search or Monte Carlo techniques. Programs such as CONFORT may offer such abilities in the future.[51]

To validate our assumption that a local minimum structure is close enough to the true bioactive conformation in ligand−protein complexes, a comparison for a sampling of PDB structures was performed. These results are shown in Table

2. Fourteen proteins were selected from the PDB which had a resolution of less than 2.0 Å. Because some of the proteins had multiple ligands, there were a total of 18 ligand structures. These structures spanned the range from simple sugars to pentapeptides and pentasaccharides. The number of atoms in the structures ranged from 14 to 114. Two of the protein structures, 1NSD and 4DFR, had duplicate ligand structures, so these were used as internal standards for evaluating the usefulness of the RMS and field correlation comparisons.

The X-ray structures of the ligands were minimized, and the heavy atoms (C, N, O, S & P) of the local minima were fit to their respective X-ray structures. The average RMS deviation of the minima was 0.55 Å. The low was 0.09, while the high was 1.13 Å. The two internal reference structures showed RMS deviations of 0.117 and 0.276 Å for 1NSD and 4DFR, respectively. This shows that the average RMS deviation of the minima are roughly 5- and 2-fold worse than the error seen in crystal structures themselves. The relative importance of these differences can be deceiving as is shown by an analysis of the field correlations.

The correlation coefficients for the steric (R^2_S) and electrostatic (R^2_E) fields of the minimized structures versus the X-ray structures were determined. From these two correlations, the average (R^2_{avg}) field correlation was derived. The mean R^2_S of the minima was 0.92 with a high of 1.00 and a low of 0.80. The mean R^2_E was 0.85 with a high of 0.99 and a low of 0.56. The mean R^2_{avg} was 0.89 with a high of 0.99 and a low of 0.72, and 50% of the compounds had an R^2_{avg} of 0.90 or greater. This shows that overall the local minima derived from the protein bound structures are in fact very similar to the X-ray structures themselves and that the RMS deviation is not an adequate measure of similarity. This fact is underscored by examination of the two internal reference structures which showed R^2_{avg}'s of 0.86 and 0.98 for 1NSD and 4DFR, respectively, despite the fact that the RMS deviation of the 4DFR structure is more than twice the RMS deviation of 1NSD. Examination of the 1NSD structure provides an explanation.

The 1NSD structure was the only entry for which the ligand had hydrogens. Comparison of the two separate ligand structures showed that in the reference compound one of its hydroxyl groups was pointing in the opposite direction. This is reflected in the low R^2_E of 0.73 which is sensitive to such a change, while the RMS deviation and the R^2_S are not because they only compare the heavy atoms in the structures. Not surprisingly, the RMS deviation and the R^2_S are correlated themselves ($R^2 = 0.85$), while R^2_E is not correlated to the RMS deviation ($R^2 = 0.28$). As expected, the correlation between R^2_{avg} and the RMS deviation is poor ($R^2 = 0.58$). Other compounds in the study demonstrated the same trend as the internal standards. The local minimum of the ligand from 1JET had a relatively large RMS deviation of 0.776 Å but a high R^2_{avg} of 0.90. The local minima of ligands from 1MMQ, 1ONE(b), 1SHA, and 3XIS(a) all had significantly lower RMS deviations (0.530, 0.666, 0.583, 0.381 Å), while their R^2_{avg} values were all lower (0.86, 0.78, 0.85, 0.88). Thus, the field correlation coefficients provide a more interpretable and accurate standard for comparing different compounds than do RMS deviations. Also, we have demonstrated that local minima on the gas phase potential energy surface are reasonably close approximations to the protein bound conformations.

To validate our ability to find a local minimum which is close to the protein bound structure, a complete systematic search was performed on two of the small molecule ligands, methotrexate from 4DFR and chloramphenicol from 3CLA. Potential energy surfaces with 4488 and 425 588 conformers were generated for chloramphenicol and methotrexate, respectively, on which 194 and 1977 local minima were located. The previous minimizations were done without electrostatics so as not to overemphasize intramolecular interactions. The minimizations of the local minima from the search surface were done with electrostatics and a distance dependent dielectric of 2.0*R. In both cases, conformations close to the protein bound conformations were located, and they were almost identical to the local minima derived without electrostatics. The overlays of the most similar local minima are shown in Figure 4. The chloramphenicol structure was generated from a search of seven torsion angles at only 60°. For methotrexate it was necessary to lower three of the torsion angle increments to 30° because of steric crowding around the aniline nitrogen. Despite the crudeness of the conformational search, the best approximation of the protein bound conformation was located.

We have shown that the local minima derived in this study are close approximations of the protein bound ligand structures and that these structures can be located using systematic search methods followed by gas phase minimization. These results are contrary to those previously published by Nicklaus et al.,[52] who states that "many of the ligands are not even in any local vacuum energy minimum when complexed with the protein". This conclusion was reached by using the "local energy, i.e., the distance in energy from the nearest local minimum" to protein bound structure and RMS deviations as a point of comparison. We have already discussed the problems with RMS comparisons so we will now address the problems with the energetic arguments.

The first problem is that the real energy of interest is the free energy change that occurs when a ligand leaves the aqueous solvated environment and binds to the protein binding site. Their study only addressed the enthalpic or deformation energy of the ligand itself, and therefore, the "local energy" they describe is not balanced or attenuated by solvation and entropic changes. The second problem is their ability to calculate meaningful "local energies" using the method they described is questionable. In their own study they report energy differences of local minima from almost identical starting structures which are vastly different. Let us take methotrexate, which they studied, as an example. Two small molecule crystal structures of methotrexate (DOJAZD and DOJAZD01) were obtained from the Cambridge Structural Database, and two protein bound ligand structures were obtained from the Protein Data Bank (4DFR). We calculated the RMS deviation and R^2_S of DOJAZD fit to DOJAZD01 to be 0.090 Å and 1.00, respectively. The RMS deviation and R^2_S of the two protein bound ligands was calculated as 0.276 Å and 0.97, respectively. They, however, calculated the energy differences from the crystal conformations to the nearest local minimum conformations as 23.00 and 9.46 kcal/mol for DOJAZD and DOJAZD01 and 18.72 and 14.27 kcal/mol for the protein bound ligands. These are differences of 13.54 and 4.45 kcal/mol for

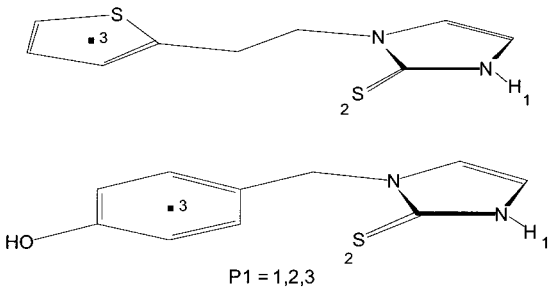

Figure 5. Postulated set of pharmacophore elements for MMD and SKF DBH inhibitors.

Table 3. Summary of LMM Results

models[a]	N[b]	comp[c]	cR^2 [d]	SECP[e]	pR^2 [f]	SEP[g]	Hres[h]	Lres[i]
MMD	12	1	−0.04	0.73	−0.04	1.01	1.87	−2.19
MMD	11	2	0.47	0.54	−0.18	1.03	1.95	−2.84
SKF	14	9	0.38	0.96	−0.01	0.99	2.71	−1.22
combined	26	4	0.47	0.62	0.05	0.84	2.37	−1.14
refined	32	4	0.51	0.65	0.71	0.41	0.74	−0.67
complete	56	5	0.73	0.46				

[a] Row definitions from Table 1: MMD = 1,2,4:12, SKF =13:26, combined = 1:26, refined = 1:32). [b] N = number of observations. [c] Comp = number of components. [d] cR^2 = cross-validated R^2. [e] SECP = standard error of cross-validated predictions. [f] pR^2 = predictive R^2. [g] SEP = standard error of predictions. [h] Hres = highest positive residual. [i] Lres = lowest negative residual.

structures derived from nearly identical starting geometries. These large differences show that the energies calculated by their method are not a reliable metric for judging differences between protein bound and local minimum conformations because they are not even self-consistent. It also demonstrates that small deviations in bond lengths and bond angles can result in very large changes in force field derived energies that are not necessarily reflected in significant changes in the geometries of the structures.

Additionally, we were not able to reproduce the folded structure of the methotrexate local minimum as reported in their study. Instead we found the one shown in Figure 4. We speculate that part of the reason for this difference is that we used a distance dependent dielectric of 2.0**R* to better mimic a protein environment while they used a vacuum dielectric constant of 1.0 and that differences in the atomic partial charges could also contribute to modulating the relative importance of electrostatic interactions versus the internal strain energy of the compounds.

The strategy employed in testing the local minima method was to first apply it to a very small data set similar in scope to what one may have at the outset of a new project. Therefore, the MMD data set was the first to be examined (Table 1, rows 1−12). The reference compound chosen was the 2-(thienylethyl)-imidazole-2(3*H*)-thione (Figure 5) which is compound **1** in Table 1. The pharmacophore elements chosen were the hydrogen on the imidazole nitrogen, the thione sulfur, and the centroid of the thiophene ring. The results of the best statistical models are shown in Table 3. The MMD models were used to predict rows 13−56 (Table 1). An acceptable cR^2 (cross-validated R^2) value of 0.47 was found when the only difluoro-phenyl compound (**3**) was omitted.

The second set of data examined were the SKF para-substituted phenylalkyl-imidazole-2(3*H*)-thiones. These compounds are rows 13−26 in Table 1. Compound **1** was still used as the reference compound for creating the alignments; however, it was not included in the CoMFA calculations. Figure 5 shows the corresponding set of pharmacophore elements used in the alignment procedure. The SKF model was used to predict rows 27−56. Its cR^2 value of 0.38 was a bit low, and neither the MMD or SKF model were predictive as indicated by their negative pR^2 (predictive R^2) values, so the data sets were combined.

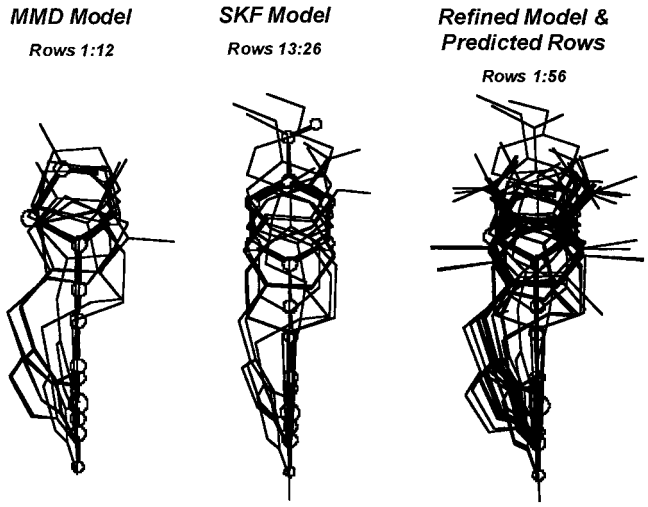

Figure 6. An overlay of compounds according to the optimal LMM pharmacophore. Compound **1** is highlighted as a ball-and-stick rendition in the MMD and Refined models. Compound **16** is highlighted as a ball-and-stick rendition in the SKF model.

The combined model was used to predict rows 27−56. The cR^2 value of 0.47 was reasonable, but the pR^2 value of 0.05 was still too low. As may be expected for two narrowly defined series, a model with good self-consistency was found but it was not predictive. The prediction data set was much more varied in the types of substitutions on the aromatic ring. To correct this problem, all compounds predicted by the combined model with absolute residuals > 1.0 were included in the refined model.

The refined model was used to predict rows 33−56. This resulted in a self-consistent model (cR^2 = 0.51) which was highly predictive (pR^2 = 0.71). Predictions and residuals from the refined model are shown in Table 1. The highest positive residual was 0.74, while the lowest negative residual was −0.67. Out of the 24 predicted compounds, seven had negative residuals while 17 had positive residuals. This indicated that the refined model still tended to overestimate its predictions. The complete model was created by including all 56 compounds and doing only full cross-validation. This resulted in a significant improvement in the cross-validated statistics (cR^2 = 0.73) over the refined model. The non-cross-validated statistics were as follows for (1) the refined model: N = 32, R^2 = 0.91, SE = 0.28, F = 69.65, P < 0.00, Comp = 4, and (2) the complete model: N = 56, R^2 = 0.91, SE = 0.26, F = 105.58, P < 0.00, Comp = 5.

Figure 6 shows a series of overlays for compounds in the MMD, SKF, and refined models. The overlay is interesting in that it shows a good match of the hydrogens on the imidazole nitrogens and the thione sulfurs where the distance to the Cu^+ atoms would be critical. The centroids of the aromatic rings, on the other hand, are allowed more freedom to position themselves at the putative phenolic region of the

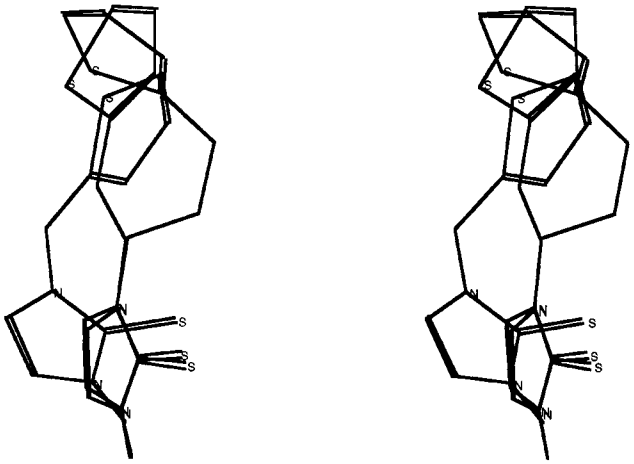

Figure 7. Overlay of three MMD 2-thienylalkyl DBH inhibitors based on the refined model (relaxed stereo).

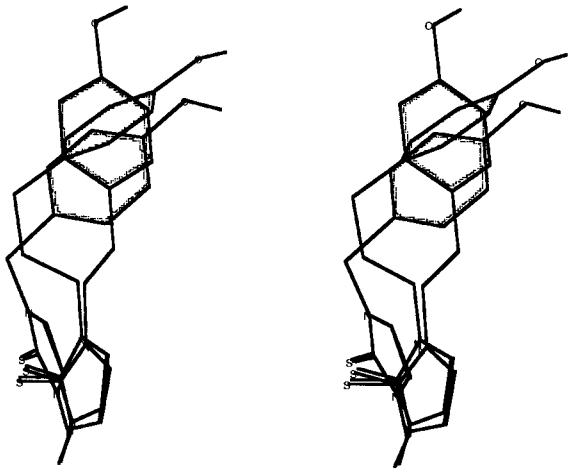

Figure 8. Overlay of three SKF 4-OH-phenylalkyl DBH inhibitors according to the refined model (relaxed stereo).

active site where the exact distances for hydrophobic or π-stacking interactions should be less critical. Figure 7 above shows the 1-, 2-, and 3-methylene 2-thiophene compounds overlayed according to the refined model. Notice the similar position of the sulfur in the three thiophene rings. According to the MNDO point charges, the sulfurs in the thiophene rings have a net positive charge plus more steric bulk. Both the steric and electrostatic contours of the CoMFA fields show these features of the molecules to have a positive contribution toward their activity. Figure 8 shows the overlay of three SKF inhibitors. Notice the position and orientation of the para-hydroxy group on the methyl and propyl bridged compounds. They are in the same region of 3D space, and they point in the same direction, possibly toward a hydrogen bond acceptor site in the enzyme. This explains their 1 order of magnitude better IC_{50}'s compared to the ethyl bridged compound.

The details of the generalized pharmacophore for DBH inhibitors based on the refined model are shown in Table 4. Two different sets of pharmacophore statistics were compiled. These were based on the number of methylene units (or equivalent) connecting the two rings. The first set included all of the compounds, while the second used only compounds with 1−3 methylene units. The second set of statistics is probably more relevant for high activity compounds.

Table 4. Generalized Pharmacophore for DBH Inhibitors

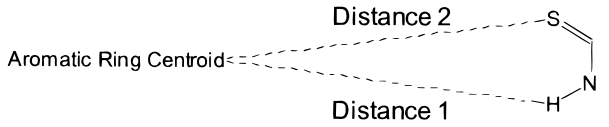

distance	no. of methylenes	mean (Å)	sd dev (Å)	high (Å)	low (Å)
1	0 to 5	6.78	1.12	10.85	5.69
2	0 to 5	5.61	1.04	9.47	4.07
1	1 to 3	6.67	0.91	8.28	5.78
2	1 to 3	5.53	0.81	7.07	4.07

Table 5. Thiophene as a Bioisostere of Phenyl

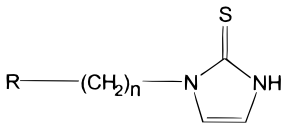

R	IC_{50} (μM) $n=1$	$n=2$	$n=3$	data source
2-thienyl	27	0.65	11	corrected MMD
phenyl	32	(5.5)[a]	16	measured SKF
4-OH-phenyl	2.6	23	2.2	measured SKF

[a] Predicted value from the refined model.

The pharmacophore consists of a *cis*-thioamide and an aromatic ring centroid (Table 4). Distance 1 is from the thioamidic hydrogen to the aromatic ring centroid. Distance 2 is from the thione sulfur to the aromatic ring centroid. In all of the compounds examined in this study, the thioamide group was part of an imidazole-2(3*H*)-thione ring. Since no substitutions or different ring systems were used, this portion of the enzyme active site was not explored by this model except for variations due to the position of the imidazole-2(3*H*)-thione ring.

Alternatively, the oxygen mimic can be considered to be in the thiol form. For this case, the thioamidic hydrogen in the pharmacophore would be replaced by a lone pair of electrons on the nitrogen. Using the lone pair (defined to be 1.0 Å from the nitrogen), the thiol sulfur, and the aromatic ring centroid as the postulated set of pharmacophore elements would have produced basically the same results. This is because the regression technique can only correlate variation in the activity data (the IC_{50}'s) with variation in the molecular descriptors (the steric and electrostatic fields). Therefore, whenever a portion of an inhibitor remains constant throughout a series of molecules, its contribution to the activity calculated by the QSAR equation will be zero.

Thiophene is generally considered to be a bioisostere of phenyl.[19] In the paper by McCarthy et al.,[20] which discussed the MMD series of inhibitors, it was speculated that thiophene may not be acting as a bioisostere because of conformational differences between thiophene and 4-hydroxy-phenyl based inhibitors in their postulated bioactive conformations. The compounds and their activities are listed in Table 5. In the 2-thienyl series, the compound with a 2-methylene linker exhibited the greatest potency. The trend in the 4-OH-phenyl series was the opposite with the 2-methylene linker having the least potency. The 2-methylene compound in the phenyl series was never made. However, it was predicted by the refined model to have the

best potency in the series. This is the same trend as that seen for the 2-thienyl series and is in agreement with the notion that thiophene is a bioisostere of phenyl. In fact, all of the values differ by a constant of only 5 μM.

The change in this trend for the 4-OH-phenyl series is due to the spatial disposition of the OH groups according to the refined model. The electrostatic CoMFA field indicates that the OH on the ethyl bridged compound is in an unfavorable location, while the methyl and propyl bridged compounds place their OH's in favorable locations. A stereoview of the three SKF 4-hydroxy-phenyl compounds overlayed according to the refined model is shown in Figure 8. Notice that the hydroxyls on both the 4-OH-phenylmethyl and the 4-OH-phenylpropyl compounds point in the same direction, possibly toward a hydrogen bond acceptor site on the enzyme. The hydroxyl on the 4-OH-phenylethyl compound is not in the same location, and therefore, it misses this positive interaction. This accounts for the activity trends shown in Table 5.

Amino acid residues presumed to be in the active site of DBH have also been identified by labeling with mechanism based inhibitors. These residues are Tyr 216,[25] His 249,[28] Tyr 357,[26] His 398,[27] and Tyr 477[28] (amino acid residue numbering from ref 23a). All of the labeled residues are conserved between the mouse, rat, bovine, and human sequences. As previously described (Figure 8), the refined model indicates a possible hydrogen bond acceptor site accessed by the para-hydroxyl group on the compounds 4-OH-phenylmethyl and 4-OH-phenylpropyl. The para-hydroxyphenyl groups are supposed to be binding in the tyramine substrate binding site.[16] This may also be analogous to the binding mode of *p*-cresol (4-hydroxytoluene), the mechanism based inhibitor which labeled Tyr 216. One of the hydroxyls on the three labeled tyrosines could possibly be the hydrogen bond acceptor site. Therefore, the three labeled tyrosines represent excellent candidates for site-directed mutagenesis studies. Mutation of these residues to phenylalanine followed by binding assays employing 4-OH-phenylmethyl would provide a validation of this hypothesis.

CONCLUSIONS

In this study, the PESA program has been developed for locating the various local minima on the potential energy surface of a molecule. The LMM software has also been developed. It utilizes the output of the PESA program for the local minima method of pharmacophore determination. The local minima method is rigorous and systematic. It produces a series of possible pharmacophores from a postulated set of pharmacophore elements. One can postulate as many different sets of pharmacophore elements as is desired. The best pharmacophore is then determined by performing a comparative molecular field analysis on each one. The pharmacophore which produces the most self-consistent model or the most predictive model (if test data are available) is deemed the best.

The two major assumptions of the method were validated by studying a sampling of ligand−protein complexes from the Protein Data Bank. We demonstrated that field correlation coefficients provide a more interpretable and accurate standard for comparing different compounds than do RMS deviations and energetic comparisons. Also, we have demonstrated that local minima on the gas-phase potential energy surface are reasonably close approximations to the protein bound conformations and that these conformations can be found through systematic conformational searches followed by minimization of the local minima on the rigid rotor search surface.

The local minima method was then applied in a series of computational experiments, and an optimal pharmacophore was determined for a series DBH inhibitors using their IC_{50} values and the maximum molecular volume overlap selection criterion. This pharmacophore produced a QSAR model based on the CoMFA steric and electrostatic fields which was highly predictive ($pR^2 = 0.71$ and SEP $= 0.41$). The model predicted that the phenyl and thienyl series were acting as bioisosteres with the one, two, and three methylene bridged compounds showing maximum potency with the two methylene linker in the unsubstituted aromatic ring systems. Examination of the alignment of compounds in the model indicated a possible hydrogen bond acceptor in the DBH active site. One of the three tyrosine residues previously labeled by mechanism based inhibitors may be acting as the acceptor, and therefore, these residues are excellent candidates for site-directed mutagenesis studies.

ACKNOWLEDGMENT

The authors thank Dr. Eugene A. Coats, Dr. Bobby Barnett, and Dr. Kenneth M. Blumenthal for their involvement in David A. Demeter's Ph.D. program as well as Marion Merrell Dow Inc. and the R.W. Johnson Pharmaceutical Research Institute whose computing facilities were made available for the completion of this work.

REFERENCES AND NOTES

(1) Demeter, D. A. Development and Application of Potential Energy Surface Analysis and the Local Minima Method of Pharmacophore Determination. Ph.D. Dissertation, University of Cincinnati, 1994; pp 1−179.

(2) (a) Villafranca, J. J.; Ash, D. E.; Colombo, G.; Fitzpatrick, P. F.; Papadopoulos, N. J.; Rajashekhar, B. *Molecular Architecture of Proteins and Enzymes*; Bradshaw, R. A., Tang, J., Eds.; Academic Press: Orlando, FL, 1985; pp 31−50. (b) Stewart, L. C.; Klinman, J. P. Dopamine β-hydroxylase of adrenal chromaffin granules: structure and function. *Annu. Rev. Biochem.* **1988**, *57*, 551−592. (c) Ash, D. E.; Papadopoulos, N. J.; Colombo, G.; Villafranca, J. J. Kinetic and spectroscopic studies of the interaction of copper with dopamine β-hydroxylase. *J. Biol. Chem.* **1984**, *259*, 3395−3398. (d) Klinman, J. P.; Krueger, M.; Brenner, M.; Edmondson, D. E. Evidence for two copper atoms/subunit in dopamine β-monooxygenase catalysis. *J. Biol. Chem.* **1984**, *259*, 3399−3402.

(3) Oka, M.; Kijikawa, K.; Ohuchi, T.; Yoshida, H.; Imaizumi, R. Distribution of dopamine-β-hydroxylase in subcellular fractions of adrenal medulla. *Life Sci.* **1967**, *6*, 461−465.

(4) Stjarne, L.; Lishajko, F. Localization of different steps in noradrenaline synthesis to different fractions of a bovine splenic nerve homogenate. *Biochem. Pharmacol.* **1967**, *16*, 1719−1728.

(5) Brenner, M. C.; Klinman, J. P. Correlation of Copper Valency with Product Formation in Single Turnovers of Dopamine β-Monooxygenase. *Biochemistry* **1989**, *28*, 4664−4670.

(6) Klinman, J. P.; Dooley, D. M.; Duine, J. A.; Knowles, P. F.; Mondovi, B.; Villafranca, J. J. Status of the cofactor identity in copper oxidative enzymes. *FEBS Lett.* **1991**, *282*, 1−4.

(7) DeWolf, W. E., Jr.; Chambers, P. A.; Southan, C.; Saunders, D.; Kruse, L. I. Inactivation of Dopamine β-Hydroxylase by β-Ethynyltyramine: Kinetic Characterization and Covalent Modification of an Active Site Peptide. *Biochemistry* **1989**, *29*, 3833−3842.

(8) (a) Rosenberg, R. C.; Lovenberg, W. Dopamine-β-hydroxylase. *Essays Neurochem. Neuropharm.* **1980**, *4*, 163−209. (b) Ljones, T.; Skotland, T. *Copper Proteins and Copper Enzymes*; Lontie, R., Ed.; CRC Press: Boca Raton, FL, 1984; Vol. 2, p 131. (c) Villafranca, J. J. *Copper Proteins*; Spiro, T. G., Ed.; Wiley: New York, 1981; p 264.

(9) (a) Axelrod, J. Dopamine-β-hydroxylase. Regulation of its synthesis and release from nerve terminals. *Pharmacol. Rev.* **1972**, *24*, 233−243. (b) Sole, M. J.; Kamble, A. B.; Hussian, M. N. A Possible Change in the Rate Limiting Step for Cardiac Norepinephrine Synthesis in the Cardiomyopathic Syrian Hamster. *Circ. Res.* **1977**, *41*, 814−817.

(10) (a) DeChamplain, J.; Farley, L.; Cousineau, D.; Ameringen, M. R. van, Circulating catechol amine levels in human and experimental hypertension. *Circ. Res.* **1976**, *38*, 109−114. (b) DeQuattro, V.; Chan, S. Raised plasma-catecholamines in some patients with primary hypertension. *Lancet* **1972**, *1*, 806−809. (c) Engelman, K.; Portnoy, B.; Sjoerdsma, A. Plasma catechol amine concentrations in patients with hypertension. *Circ. Res., Suppl.* **1970**, *27*, 141−146. (d) Franco-Morselli, R.; Elghozi, J. L.; Joly, E.; Di Giuilio, S.; Meyer, P. Increased plasma adrenaline concentrations in benign essential hypertension. *Br. Med. J.* **1977**, *2*, 1251−1254. (e) Goldstein, D. S. Plasma norepinephrine in essential hypertension. A study of the studies. *Hypertension* **1981**, *3*, 48−52. (f) Louis, W. J.; Doyle, A. E.; Anavekar, S. Plasma norepinephrine levels in essential hyoertension. *N. Engl. J. Med.* **1973**, *288*, 599−601. (g) Nagatsu, T.; Ikuta, K.; Numata (Sudo), Y.; Kato, T.; Sano, M.; Nagatsu, I.; Umezawa, H.; Matsuzaki, M.; Takeuchi, T. Vascular and brain dopamine β-hydroxylase activity in young spontaneously hypertensive rats. *Science (Washington, D.C.)* **1976**, *191*, 290−291. (h) Fujita, K.; Teradaira, R.; Inoue, T.; Takahashi, H.; Beppu, H.; Kawai, K.; Maruta, K.; Yagyo, S.; Nagatsu, T. Stress-induced changes in in vivo and in vitro dopamine-β-hydroxylase activity in spontaneously hypertensive rats. *Biochem. Med.* **1982**, *28*, 340−346.

(11) Chidsey, C. A.; Sonnenblick, E. H.; Morrow, A. G.; Braunwald, E. Norepinephrine stores and contractile force of papillary muscle from the failing human heart. *Circulation* **1966**, *33*, 43−51.

(12) Ohlstein, E. H.; Kruse, L. I.; Ezekiel, M.; Sherman, S. S.; Erickson, R.; DeWolf, W. E., Jr.; Berkowitz, B. A. Cardiovascular effects of a new potent dopamine β-hydroxylase inhibitor in spontaneously hypertensive rats. *J. Phamacol. Exp. Ther.* **1987**, *241*, 554−559.

(13) (a) Kruse, L. I.; Kaiser, C.; DeWolf, W. E., Jr.; Chambers, P. A.; Goodhart, P. J.; Ezekiel, M.; Ohlstein, E. H. β-Substituted Phenethylamines as High-Affinity Mechanism-Based Inhibitors of Dopamine β-Hydroxylase *J. Med. Chem.* **1988**, *31*, 704−706. (b) Fitzpatrick, P. F.; Villafranca, J. J. Mechanism-based inhibitors of dopamine β-hydroxylase. *Arch. Biochem. Biophys.* **1987**, *257*, 231−250. (c) May, S. W.; Wimalasena, K.; Herman, H. H.; Fowler, L. C.; Ciccarello, M. C.; Pollock, S. H. Novel antihypertensives targeted at dopamine β-monooxygenase: turnover-dependent cofactor depletion by phenyl aminoethyl selenide. *J. Med. Chem.* **1988**, *31*, 1066−1068.

(14) Kruse, L. I.; DeWolf Jr., W. E.; Chambers, P. A.; Goodhart, P. J. Design and Kinetic Characterization of Multisubstrate Inhibitors of Dopamine β-Hydroxylase. *Biochemistry* **1986**, *25*, 7271−7278.

(15) Kruse, L. I.; Kaiser, C.; DeWolf, W. E., Jr.; Frazee, J. S.; Garvey, E.; Hilbert, E. L.; Faulkner, W. A.; Flaim, K. E.; Sawyer, J. L.; Berkowitz, B. A. Multisubstrate inhibitors of Dopamine β-Hydroxylase. 1. Some 1-Phenyl and 1-Phenyl-Bridged Derivatives of Imidazole-2-thione. *J. Med. Chem.* **1986**, *29*, 2465−2472.

(16) Kruse, L. I.; Kaiser, C.; DeWolf, W. E., Jr.; Frazee, J. S.; Ross, S. T.; Wawro, J.; Wise, M.; Flaim, K. E.; Sawyer, J. L.; Erickson, R. W.; Ezekiel, M.; Ohlstein, E. H.; Berkowitz, B. A. Multisubstrate Inhibitors of Dopamine β-Hydroxylase. 2. Structure−Activity relationships at the Phenethylamine Binding Site. *J. Med. Chem.* **1987**, *30*, 486-494.

(17) Ross, S. T.; Kruse, L. I.; Ohlstein, E. H.; Erickson, R. W.; Ezekiel, M.; Flaim, K. E.; Sawyer, J. L.; Berkowitz, B. A. Inhibitors of Dopamine β-Hydroxylase. 3. Some 1-(Pyridylmethyl)imidazole-2-thiones. *J. Med. Chem.* **1987**, *30*, 1309−1313.

(18) Kruse, L. I.; Kaiser, C.; DeWolf, W. E.; Finkelstein, J. A.; Frazee, J. S.; Hilbert, E. L.; Ross, S. T.; Flaim, K. E.; Sawyer, J. L. Some Benzyl-Substituted Imidazoles, Triazoles, Tetrazoles, Pyridinethiones, and Structural Relatives as Multisubstrate Inhibitors of Dopamine β-Hydroxylase. 4. Structure−Activity Relationships at the Copper Binding Site. *J. Med. Chem.* **1990**, *33*, 781−789.

(19) Press: J. B. Pharmacologically Active Compounds and Other Thiophene Derivatives. In *Thiophene and Its Derivatives*; Gronowitz, S., Ed.; Wiley: New York, 1985; Vol. 44, Part 1, pp 353−456.

(20) McCarthy, J. R.; Matthews, D. P.; Broersma, R. J.; McDermott, R. D.; Kastner, P. R.; Hornsperger, J.-M.; Demeter, D. A.; Weintraub, H. J. R.; Whitten, J. P. 1-(Thienylalkyl)imidazole-2(3H)-thiones as Potent Competitive Inhibitors of Dopamine β-Hydroxylase. *J. Med. Chem.* **1990**, *33*, 1866−1873.

(21) Nakano, T.; Kobayashi, K.; Saito, S.; Fujita, K.; Nagatsu, T. Mouse dopamine β-hydroxylase: primary stucture deduced from the cDNA sequence and exon/intron organization of the gene. *Biochem. Biophys. Res. Commun.* **1992**, *189*, 590−599.

(22) .McMahon, A.; Geertman, R.; Sabban, E. L. Rat dopamine β-hydroxylase: molecular cloning and characterization of the cDNA and regulation of the mRNA by resperine. *J. Neurosci. Res.* **1990**, *25*, 395−404.

(23) (a) Wang, N.; Southan, C.; DeWolf, W. E., Jr.; Wells, T. N.; Kruse, L. I.; Leatherbarrow, R. J. Bovine dopamine β-hydroxylase, primary structure determined by cDNA cloning and amino acid sequencing. *Biochemistry* **1990**, *29*, 6466−6474. (b) Wu, H. J.; Parmer, R. J.; Koop, A. H.; Rozansky, D. J.; O'Connor, D. T. Molecular cloning, structure, and expression of dopamine β-hydroxylase from bovine adrenal medulla. *Journal of Neurochemistry* **1990**, *55*, 97−105. (c) Robertson, J. G.; Desai, P. R.; Kumar, A.; Farrington, G. K.; Fitzpatrick, P. F.; Villafranca, J. J. Primary amino acid sequence of bovine dopamine β-hydroxylase. *J. Biol. Chem.* **1990**, *265*, 1029−1035. (d) Lewis, E. J.; Allison, S.; Fader, D.; Claflin, V.; Baizer, L. Bovine dopamine β-hydroxylase cDNA. Complete coding sequence and expression in mammalian cells with vaccinia virus vector. *J. Biol. Chem.* **1990**, *265*, 1021−1028.

(24) (a) Kobayashi, K.; Kurosawa, Y.; Fujita, K.; Nagatsu, T. Human dopamine β-hydroxylase gene: two mRNA types having different 3′-terminal regions are produced through alternative polyadenylation. *Nucleic Acids Research* **1989**, *17*, 1089−1102. (b) Lamouroux, A.; Vigny, A.; Faucon Biguet, N.; Darmon, M. C.; Franck, R.; Henry, J. P.; Mallet, J. The primary structure of human dopamine β-hydroxylase: insights into the relationship between the soluble and the membrane-bound forms of the enzyme. *EMBO Journal* **1987**, *6*, 3931−3937.

(25) DeWolf, W. E., Jr.; Carr, S. A.; Varrichio, A.; Goodhart, P. J.; Mentzer, M. A.; Roberts, G. D.; Southan, C.; Dolle, R. E.; Kruse, L. I. Inactivation of Dopamine β-Hydroxylase by *p*-Cresol: Isolation and Characterization of Covalently Modified Active Site Peptides. *Biochemistry* **1988**, *27*, 9093−9101.

(26) Southan, C.; DeWolf, W. E., Jr.; Kruse, L. I. Inactivation of dopamine β-hydroxylase by *p*-cresol: evidence for a second, minor site of covalent modification at tyrosine 357. *Biochim. Biophys. Acta* **1990**, *1037*, 256−258.

(27) DeWolf, W. E., Jr.; Chambers, P. A.; Southan, C.; Saunders: D.; Kruse, L. I. Inactivation of Dopamine β-Hydroxylase by β-Ethynyltyramine: Kinetic Characterization and Covalent Modification of an Active Site Peptide. *Biochemistry* **1989**, *28*, 3833−3842.

(28) Farrington, G. K.; Kumar, A.; Villafranca, J. J. Active Site Labeling of Dopamine β-Hydroxylase by Two Mechanism-based Inhibitors: 6-Hydroxybenzofuran and Phenylhydrazine. *J. Biol. Chem.* **1990**, *265*, 1036−1040.

(29) Tainer, J. A.; Getzoff, E. D.; Beem, K. M.; Richardson, J. S.; Richardson, D. C. Determination and analysis of the 2 Å structure of copper, zinc superoxide dismutase. *J. Mol. Biol.* **1982**, *160*, 181−217.

(30) Robertson, J. G.; Desai, P. R.; Kumar, A.; Farrington, G. K.; Fitzpatrick, P. F.; Villafranca, J. J. Primary amino acid sequence of bovine dopamine β-hydroxylase. *J. Biol. Chem.* **1990**, *265*, 1029−1035.

(31) Pettingill, T. M.; Strange, R. W.; Blackburn, N. J. Carbonmonoxy Dopamine β-Hydroxylase: Structural Characterization by Fourier Transform Infrared, Fluorescence, and X-ray Absorption Spectroscopy. *J. Biol. Chem.* **1991**, *266*, 16996−17003.

(32) Blackburn, N. J.; Hasnain, S. S.; Pettingill, T. M.; Strange, R. W. Copper *K*-Extended X-ray Absorption Fine Structure Studies of Oxidized and Reduced Dopamine β-Hydroxylase. *J. Biol. Chem.* **1991**, *266*, 23120−23127.

(33) Scott, R. A.; Sullivan, R. J.; DeWolf, W. E., Jr.; Dolle, R. E.; Kruse, L. I. The Copper Sites of Dopamine β-Hydroxylase: An X-ray Absorption Spectroscopic Study. *Biochemistry* **1988**, *27*, 5411−5417.

(34) Blumberg, W. E.; Desai, P. R.; Powers, L.; Freedman, J. H.; Villafranca, J. J. X-ray Absorption Spectroscopic Study of the Active Copper Sites in Dopamine β-Hydroxylase. *J. Biol. Chem.* **1989**, *264*, 6029−6032.

(35) McCracken, J.; Desai, P. R.; Papadopoulos, N. J.; Villafranca, J. J.; Peisach, J. Electron spin−echo studies of the copper(II) binding sites in dopamine β-hydroxylase. *Biochemistry* **1988**, *27*, 4133−4137.

(36) Blackburn, N. J.; Pettingill, T. M.; Seagraves, K. S.; Shigeta, R. T. Characterization of a carbon monxide complex of reduced dopamine β-hydroxylase. Evidence for inequivalence of the Cu(I) centers. *J. Biol. Chem.* **1990**, *265*, 15383−15386.

(37) Farger, L. Y.; Alben, J. O. Structure of the carbon monoxide binding site of hemocyanins studied by Fourier transform infrared spectroscopy. *Biochemistry* **1972**, *11*, 4786−4792.

(38) (a) Volbeda, A.; Hol, W. G. J. Crystal structure of hexameric haemocyanin from Panulirus interruptus refined at 3.2 Å resolution. *J. Mol. Biol.* **1989**, *209*, 249−279. (b) Solomon, E. I. In *Metal Ions in Biology*; Spiro, T. G., Ed.; John Wiley & Sons: New York, 1981; pp 40−108.

(39) (a) Marshall, G. R.; Barry, C. D.; Bosshard, H. E.; Dammkoehler, R. A.; Dunn, D. A. The conformational parameter in drug design: the active analogue approach. In *Computer Assisted Drug Design*; Olson, E. C., Christofferson, R. E., Eds.; American Chemical Society: ACS Symposium Series, Washington, D.C., 1979; Vol. 112, pp 205−226.

(b) Mayer, D.; Naylor, C. B.; Motoc, I.; Marshall, G. R. A unique geometry of the active site of angiotensin-converting enzyme consistent with structure−activity studies. *J. Comput.-Aided Mol. Design* **1987**, *1*, 3−16.

(40) (a) Cramer III, R. D.; Patterson, D. E.; Bunce, J. D. Comparative molecular-field analysis (COMFA). 1. Effect of shape on binding of steroids to carrier proteins. *J. Am. Chem. Soc.* **1988**, *110*, 5959−5967. (b) Marshall, G. R.; Cramer III, R. D. 3-Dimensional structure activity relationships. *Trends in Pharmacol. Sci.* **1988**, *9*, 285−289. (c) Allen, M. S.; Yan, Y. C.; Trudell, M. L.; Narayanan, K.; Schindler, L. R.; Martin, M. J.; Schultz, C.; Hagen, T. J.; Koehler, K. F.; Codding, P. W.; Skolnick, P.; Cook, J. M. Synthetic and computer-assisted analyses of the pharmacophore for the benzodiazepine receptor inverse agonist site. *J. Med. Chem.* **1990**, *33*, 2343−2357.

(41) Dunn, W. J.; Wold, S.; Edlund, U.; Hellberg, S. Multivariate Structure−Activity Relationships Between Data from a Battery of Biological Tests and an Ensemble of Structure Descriptors: The PLS Methodol. *Quant. Struct.-Act. Relat.* **1984**, *3*, 131−137.

(42) Kim, K. H. Use of Indicator Variable in Comparative Molecular Field Analysis. *Med. Chem. Res.* **1993**, *3*, 257−267.

(43) Tripos Associates, 1699 S. Hanley Road, Suite 303, St. Louis, MO 63144.

(44) (a) Clark, M.; Cramer III, R. D.; Van Opdenbosch, N. Validation of the General Purpose Tripos 5.2 Force Field. *J. Comput. Chem.* **1989**, *10*(8), 982−1012. (b) Sybyl 6.0 Theory Manual, Appendix 2.2, pp 2421−2423, October 1992.

(45) Dewar, M. J. S.; Thiel, W. Ground-states of molecules. 38. MNDO Method − approximations and parameters. *J. Am. Chem. Soc.* **1977**, *99*, 4899−4907.

(46) Stewart, J. J. P. MOPAC 5.0, QCPE program no. 455.

(47) Clark, D. E.; Willett, P.; Kenny, P. W. Pharmacophoric pattern matching in files of three-dimensional chemical structures: Use of bounded distance matrixes for the representation and searching of conformationally flexible molecules. *J. Mol. Graphics* **1992**, *10*(4), 194−204.

(48) Martin, Y. C.; Bures, M. G.; Danaher, E. A.; DeLazzer, J.; Lico, I.; Pavlik, P. A. A fast approach to pharmacophore mapping and its application to dopaminergic and benzodiazepine agonists. *J. Comput.-Aided. Mol. Design.* **1993**, *7*, 83−102.

(49) Golender, V.; Vesterman, B.; Vorpagel, E. APEX-3D Expert System for Drug Design. *Network Sci.* **1996**, *2*, http://www.awod.com/netsci/Issues/Jan96/feature3.html (no pp given).

(50) (a) Sprague, P. W.; Hoffmann, R. CATALYST pharmacophore models and their utility as queries for searching 3D databases. *Comput.-Assisted Lead Find. Optim. [Eur. Symp. Quant. Struct.-Act. Relat.]*, 11th; Eds.; Van de Waterbeemd, H.; Testa, B.; Folkers, G. Verlag Helvetica Chimica Acta: Basel, Switzerland; 1997; pp 225−240. (b) Kahn, S. D.; Hahn, M.; Parish, D. The use of feature-and shape-based database searching techniques to identify new drug templates. *Book of Abstracts*, 211th ACS National Meeting, New Orleans, LA; American Chemical Society, Washington, D.C. March 24−28 1996, CINF-048. (c) Kaminski, J. J.; Rane, D. F.; Snow, M. E.; Weber, L.; Rothofsky, M. L.; Anderson, S. D.; Lin, S. L. Identification of Novel Farnesyl Protein Transferase Inhibitors Using Three-Dimensional Database Searching Methods. *J. Med. Chem.* **1997**, *40*(25), 4103−4112.

(51) Pearlman, R. S. Receptor-Relevant Chemistry Subspaces and Other Recent Advances. Presented at the *Tripos Users Group Meeting*; Somerset, NJ, May 19, 1998.

(52) Nicklaus, M. C.; Wang, S.; Driscoll, J. S.; Milne, G. W. A. Conformational Changes of Small Molecules Binding to Proteins. *Bioorg., Med. Chem.* **1995**, *3*(4), 411−428.

CI980404Z